THE JOURNAL OF PHYSICAL CHEMISTRY A LETTERS

2008, *112,* 4869–4874
Published on Web 05/07/2008

Infrared Spectroscopy of Gas Phase Benzenium Ions: Protonated Benzene and Protonated Toluene, from 750 to 3400 cm^{-1}

G. E. Douberly, A. M. Ricks, P. v. R. Schleyer, and M. A. Duncan*

Department of Chemistry, University of Georgia, Athens, Georgia 30602-2556

Received: March 7, 2008; Revised Manuscript Received: April 17, 2008

Gas phase $C_6H_7^+$ and $C_7H_9^+$ ions are studied with infrared photodissociation spectroscopy (IRPD) and the method of rare gas tagging. The ions are produced in a pulsed electric discharge supersonic expansion source from benzene or toluene precursors. We observe exclusively the formation of either the C_{2v} benzenium ion (protonated benzene) or the para isomer of the toluenium ion (protonated toluene). The infrared spectral signatures associated with each ion are established between 750 and 3400 cm^{-1}. Comparing the gas phase spectrum of the benzenium ion to the spectrum obtained in a superacid matrix [Perkampus, H. H.; Baumgarten, E. *Angew. Chem. Int. Ed.* 1964, *3*, 776], we find that the C_{2v} structure of the gas phase species is minimally affected by the matrix environment. An intense band near 1610 cm^{-1} is observed for both ions and is indicative of the allylic π-electron density associated with the six membered ring in these systems. This spectral signature, also observed for alkyl substituted benzenium ions and protonated naphthalene, compares favorably with the interstellar, unidentified infrared emission band near 6.2 μm (1613 cm^{-1}).

Introduction

Reactions of electrophiles with aromatic compounds have been investigated extensively in both the gas and condensed phases, resulting in one of the most thoroughly understood classes of organic reactions. It is well accepted that electrophilic aromatic substitution (EAS) reactions proceed through cyclohexadienyl cation intermediates (σ-complexes, arenium ions).[1] Many of the cations implicated as EAS reaction intermediates were isolated in either superacid solutions or matrices and examined with NMR,[2,3] IR,[4] and UV spectroscopies,[5] including the prototype $C_6H_7^+$ benzenium ion (*i.e.*, protonated benzene).[3b–d,4] The production and reactivity of benzenium and alkyl substituted benzenium ions have also been studied in the gas phase using mass spectrometers.[6] Both the gas and condensed phase studies are consistent with structures corresponding to σ-complexes (**1**). Spectroscopy of these species in the gas phase had been limited to a low resolution UV study of $C_6H_7^+$.[7] More recently, Dopfer and co-workers studied the interaction of arenium ions with various ligands using IR photodissociation spectroscopy in the C−H stretching region,[8] and Maître and co-workers examined the IR spectral signatures of the benzenium ion in the fingerprint region.[9] The IR spectral signatures of these ions are of particular interest due to the demonstrated stability and predicted abundance of protonated benzene and protonated polycyclic aromatic hydrocarbons (PAHs) in diffuse interstellar gas clouds.[10,11] We present here a comprehensive examination of the IR spectra for the benzenium and toluenium ions isolated in the gas phase.

As early as 1928, Pfeiffer and Wizinger had proposed a mechanism for EAS reactions that involved the arenium, σ-complex cation as the intermediate.[12] The earliest theoretical work by Wheland and Mulliken also supported this mechanism.[13,14] The isolation of methyl substituted benzenium ions in acidic HF/BF_3 solutions was first achieved in 1951 by Lien and McCaulay.[15] Thereafter, several UV studies of these ions in acidic solution provided some evidence for the sp^3 hybridized ring carbon atom and hence ring protonation leading to the σ-complex.[5] A more definitive structural characterization of these cations was provided by NMR.[2,3] The first NMR studies were plagued by proton exchange between the arenium ions and the acidic solvent.[2] However, this problem was avoided in the seminal work of Olah who isolated alkyl benzenium ions as hexafluoroantimonate salts.[3] Olah observed a broad resonance in the low temperature ^1H NMR near $\delta(4-5)$ characteristic of aliphatic hydrogens attached to a ring carbon atom with sp^3 hybridization.[3a] An unequivocal structural determination for the $C_6H_7^+$ benzenium ion was achieved with ^{13}C FT-NMR in 1978.[3d] At room temperature, the spectrum consists of a single peak at δ ^{13}C 145.9, corresponding to six equivalent carbon atoms resulting from the rapid intramolecular exchange of seven equivalent hydrogen atoms. However, at 139 K, characteristic resonances appear for the sp^3 hybridized carbon and the sp^2 carbons ortho, meta, and para to the CH_2 group, which indicate a planar, C_{2v} structure. Olah and co-workers noted that, from the ^{13}C chemical shifts, the positive charge in the static benzenium ion is distributed uniformly over the ortho and para carbon atoms, with a minimal buildup of charge at the meta positions. Consequently, they concluded that the π electron density in the benzenium ion is allylic.

The NMR structural characterization of the benzenium and alkyl substituted benzenium ions was completely consistent with the highest levels of *ab initio* theory at that time.[16] High levels of modern *ab initio* theory have now been brought to bear on the structure of protonated benzene,[17] all of which predict the planar C_{2v} structure observed in the superacid matrix experiments as well as the observed ^{13}C NMR chemical shifts.[17a] In fact, the ring protonated C_{2v} structure is the only minimum,

* Corresponding author. E-mail: maduncan@uga.edu.

10.1021/jp802020n CCC: $40.75

whereas the C_s edge protonated structure corresponds to the transition state for intramolecular proton exchange. Additionally, the C_{6v} face protonated π-complex is a second-order saddle point lying 47.6 kcal/mol higher in energy than the C_{2v} global minimum.[17c] A complex of H_2 with the phenyl cation can also be ruled out.[17e] Indeed, theory and experiments in both the gas and condensed phases are in complete agreement as to the structure of protonated benzene.

Benzenium and protonated PAH ions are predicted to be abundant in the interstellar medium. Efficient production processes are known for these species and they are stable toward photodissociation or further reaction.[10,11] Indeed, $C_6H_7^+$ ions have been measured with mass spectrometry in the ionosphere of Saturn's moon, Titan.[18] Closed shell benzenium and protonated PAH ions have also been implicated as potential carriers of the unidentified IR emission bands (UIBs) from carbon-containing interstellar gas clouds.[11,19] Therefore, sensitive spectroscopy in the fingerprint region of the mid-IR is highly desirable. We present here a detailed study of the IR spectroscopy of the benzenium and toluenium ions. We employ a broadly tunable optical parametric oscillator laser system and the method of rare gas tagging[20–24] to obtain the spectra in the 750−3400 cm^{-1} region. The ions produced here are at low temperatures (T < 100 K) such that the benzenium and toluenium ions can be described in terms of a static (σ-complex) structure. Comparing the spectra to the predictions of theory, we obtain a detailed assignment of all the IR active vibrations predicted in this spectral region.

Experimental and Theoretical Methods

Protonated benzene and protonated toluene are produced in a pulsed electric discharge supersonic expansion source that has been described in detail previously.[25] The expansion consists of the vapor pressure of benzene or toluene at 0 °C seeded in a gas mixture consisting of 20% H_2 and 80% Ar. Collisional cooling in the expansion results in ions with temperatures below 100 K.[25b] The molecular beam is collimated with a 2 mm diameter skimmer, and the cations produced in the discharge are subsequently pulse extracted into a specially designed reflectron time-of-flight mass spectrometer.[24] Depending on the employed precursor, either $C_6H_7^+$ or $C_7H_9^+$ is observed to be the most abundant ion produced. Weakly bound complexes of the protonated species with Ar are also produced. The binding energy of Ar to these ions is only ~200 cm^{-1}, and the calculated perturbation to the IR spectrum is small (see Supporting Information). Hence the weakly bound Ar atom provides an ideal leaving group for studying the benzenium and toluenium ions with IR photodissociation (IRPD) spectroscopy.[20–24] IRPD is carried out in the turning region of the reflectron field by overlapping the mass selected ion packet with the tunable output of an optical parametric oscillator (OPO) laser system (LaserVision). The OPO/OPA/$AgGaSe_2$ laser system is pumped by an injection-seeded Nd:YAG laser (Spectra Physics model PRO-230, equipped with "BeamLok"), producing tunable radiation between 700 and 4400 cm^{-1} with a bandwidth of ~1.2 cm^{-1}.[26] The pulse energy is set to approximately 1 mJ from 1200 to 3400 cm^{-1}, and approximately 100 μJ per pulse is achieved at 800 cm^{-1}. Resonant single photon absorption leads to the fragmentation of the weakly bound $C_nH_m^+Ar$ complex, producing $C_nH_m^+$ ion signals on a zero background. The parent and fragment ion signals are integrated with a digital oscilloscope (LeCroy Waverunner), and the fragment signal is normalized to the parent to correct for long-term fluctuations of the ion source. The IRPD spectra presented here were recorded by averaging the fragment ion signal for 50 laser shots (10 Hz) as the OPO tuned 0.5 cm^{-1}. For each case, the fragment ion corresponds to the elimination of Ar. Absolute calibration was achieved by measuring the opto-acoustic spectrum of CH_4 in an external gas cell in both the 1300 and 3000 cm^{-1} regions.

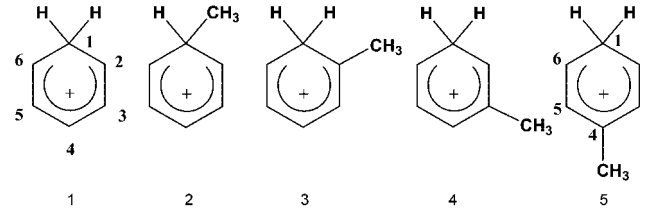

Figure 1. Structures for the (**1**) benzenium ion and the (**2**) ipso, (**3**) ortho, (**4**) meta, and (**5**) para structural isomers of the toluenium ion.

Density functional theory (DFT) computations are carried out at the B3LYP/6-311+G(d,p) level, employing the GAMESS program package.[27] Harmonic vibrational frequencies are scaled for comparison to the experiment by a factor of 0.978.[28] Calculations at the MP2 level of theory produced imaginary frequencies for $C_6H_7^+$ due to a basis set incompleteness error that has been documented and described in detail previously.[29] This error, which leads to the nonplanarity of benzene and other arenes, apparently also exists for the protonated systems. To eliminate this complication from the following discussion, we compare the experimental results to the predictions from DFT, which do not suffer from this problem.[29] The Supporting Information for this manuscript contains the full details of these calculations, including a comparison between the MP2 and DFT results, along with the structures, energetics and vibrational frequencies for each of the structures considered.

Results and Discussion

A schematic of the C_{2v} benzenium ion is shown as structure **1** in Figure 1, along with the numbering scheme used to describe the assignments of the *ab initio* normal mode vibrations presented in Table 1. Structures **2** through **5** are the four different isomers of the toluenium ion, with the para isomer (**5**) being the lowest energy structure. The IRPD spectrum of the $C_6H_7^+Ar$ ion is shown in Figure 2. The $C_6H_7^+$ B3LYP spectra, both with (blue) and without (red) Ar, are also provided for comparison. Several vibrational bands between 800 and 1700 cm^{-1} are observed, and the only other bands present between 1700 and 4400 cm^{-1} fall in the 2700−3200 cm^{-1} region. It is clear from a cursory comparison of the experimental and calculated spectra that the vast majority of $C_6H_7^+$ ions produced by our source correspond to the C_{2v} benzenium ion. Overall, below 1700 cm^{-1}, the experimental and calculated spectra are in excellent agreement. Furthermore, the perturbation of the bare benzenium ion spectrum upon complexation with Ar is minimal below 1700 cm^{-1}, with all the predicted frequency shifts being within ±10 cm^{-1}. In our previous studies of the allyl, 2-propenyl, and *tert*-butyl cations, a minimal effect due to the Ar was also observed, owing to the similarly weak complexation energies.[30]

In the fingerprint region of the $C_6H_7^+Ar$ spectrum, the band origins of the two most intense features are located at 1456 and 1607 cm^{-1}, each with a line width of 7 cm^{-1}. Both of these bands are assigned to asymmetric CCC stretch vibrations of the ring. Maître and co-workers reported the gas phase IR spectrum of $C_6H_7^+$ isolated in a 400 K ICR cell.[9] In this study, a tunable, high power free electron laser was employed to drive multiphoton dissociation (IRMPD) of the bare benzenium ion. They also observed and assigned a band in the fingerprint region

TABLE 1: IRPD Bands for Protonated Benzene ($C_6H_7^+$−Ar) Compared to the Predictions of Theory (Scaled Frequencies and Intensities in cm^{-1} (km/mol))

IRPD	*ab initio* (int)[a]	$\Delta\nu$(Ar)[b]	assignment[c]
831	828.9 (17)	+1.7	sp^3 C oop rocking; oop sp^2 CH bend
903	877.7 (14)	+2.7	sym (6,1,2) CCC str, ring breathing
964	964.1 (18)	+5.3	asym (6,1,2) CCC str; sp^3 CH_2 wag
1058	1039.4 (3)	−2.2	iph (3,5) oop CH bend, ooph with (4) oop CH bend
1198	1176.8 (18)	−10.9	asym (3,4,5) ip CH bend
	1183.0 (20)	−5.0	iph (5,6) and (2,3) CH scissor, ooph with sp^3 CH_2 scissor
1239	1255.9 (114)	−7.1	sp^3 CH_2 scissor, iph with (5,6) and (2,3) CH scissor
1334	1329.0 (15)	−1.0	asym (6,1,2) CCC str; ip sp^2 CH bend
1456	1450.2 (184)	+6.1	asym (3,4,5) CCC str
1607	1600.2 (77)	+3.3	iph asym (2,3,4) (4,5,6) CCC str
2793	2878.9 (42)	+24.2	asym sp^3 CH_2 str
2809			
2820	2887.4 (48)	−17.6	sym sp^3 CH_2 str
3006	3114.0 (3)	+3.0	asym (2,6) sp^2 CH str ooph with asym (3,5) sp^2 CH str
3035	3115.7 (5)	+3.2	sym (2,6) sp^2 CH str ooph with sym (3,4,5) sp^2 CH str
3078	3133.1 (6)	+2.3	asym (3,5) sp^2 CH str iph with asym (2,6) sp^2 CH str
3107	3135.4 (2)	+2.0	sym (2,3,4,5,6) sp^2 CH str; (3,5) largest amplitude

[a] $(C_6H_7)^+$Ar; B3LYP, 6-311+G(d,p); 0.978 scale factor. [b] *Ab initio* Ar induced frequency shift from the bare $(C_6H_7)^+$ ion. [c] Notation: in plane (ip), out of plane (oop), in phase (iph), and out of phase (ooph).

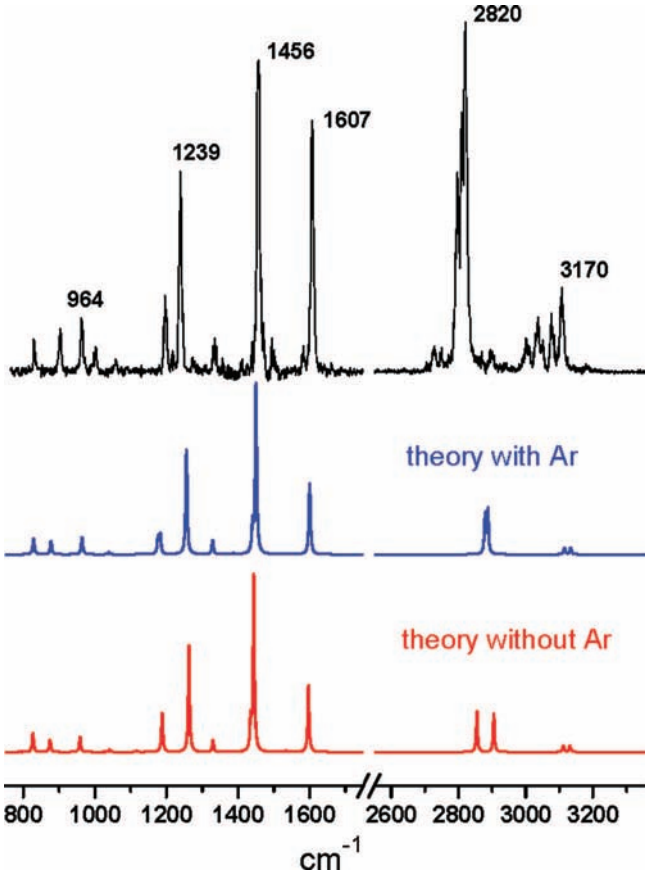

Figure 2. IR photodissociation spectrum of the $C_6H_7^+$Ar complex measured in the elimination of Ar channel. The simulated spectra from density functional calculations (B3LYP/6-311+G(d,p)) are shown for both the $C_6H_7^+$Ar complex (blue) and the bare $C_6H_7^+$ ion (red).

to a carbon ring stretch. However, the transition was 30 cm^{-1} broad and centered at 1433 cm^{-1}, corresponding to a 23 cm^{-1} red shift from the analogous band reported here. Nevertheless, this red shift discrepancy is frequently observed in IRMPD studies and originates from the anharmonic nature of the multiphoton processes leading to fragmentation.[31] We re-emphasize here that the fragmentation of the weakly bound $C_6H_7^+$Ar complex results from one photon absorption. It is also

TABLE 2: IRPD Bands for Protonated Toluene ($C_7H_9^+$−Ar) Compared to the Predictions of Theory for the Para Isomer (Scaled Frequencies and Intensities in cm^{-1} (km/mol))

IRPD	*ab initio* (int)[a]	assignment[b]
869	865.7 (19)	sp^3 CH_2 rock; iph (2,3) and (5,6) oop CH bend; methyl bend
906	883.1 (20)	sym (6,1,2) CCC str, ring breathing
980	961.0 (12)	asym (6,1,2) CCC str; sp^3 CH_2 wag; methyl bend
1028	1018.3 (29)	iph (2,3) and (5,6) oop CH bend; methyl bend
1204	1187.9 (49)	iph (2,3) and (5,6) CH scissor, (3,4,5) CCC sym str
1264		
1277	1288.4 (133)	sp^3 CH_2 scissor
1323	1315.7 (28)	ooph (2,3) and (5,6) ip CH bend; sp^3 CH_2 wag
1367	1377.4 (30)	asym (3,4,5) CCC str; methyl umbrella
1403	1419.7 (30)	ooph (2,3) and (5,6) ip CH bend; methyl bend
1473	1456.3 (50)	ooph (2,3) and (5,6) ip CH bend; methyl bend
	1459.7 (60)	(2,3) ip CH bend; methyl bend
1487	1471.2 (51)	asym (3,4,5) CCC str; methyl bend
1523	1508.7 (32)	ooph asym (6,2,1) and (3,4,5) CCC str; methyl twist
1623	1617.6 (183)	iph asym (2,3,4) and (4,5,6) CCC str
2835	2891.0 (21)	asym sp^3 CH_2 str
	2894.1 (50)	sym sp^3 CH_2 str
2914	2939.6 (33)	sym methyl CH_3 str
3068	3073.0 (4)	asym methyl CH_3 str

[a] $(C_7H_9)^+$Ar; B3LYP, 6-311+G(d,p); 0.978 scale factor. [b] Notation: in plane (ip), out of plane (oop), in phase (iph), and out of phase (ooph).

important to note that the DFT calculations predict a 6.1 cm^{-1} blue shift of this transition for the $C_6H_7^+$Ar complex (see Table 1), thereby reducing the estimated IRMPD red shift to ∼17 cm^{-1}.

The other intense transition in this region at 1607 cm^{-1} agrees well with the calculated band origin for the asymmetric CCC stretches involving the (2,3,4) and (4,5,6) carbon atoms. Considering the normal mode description for this transition, this band is similar to the 1585 cm^{-1} CCC asymmetric stretch band observed previously for the $C_3H_5^+$ allyl cation.[30b] The corresponding benzenium ion ring deformation motion is analogous to two C_3 groups oscillating asymmetrically and in phase. In light of the ^{13}C NMR data,[3d] which suggest that the π electron density in the static benzenium ion is allylic, the above description for the 1607 cm^{-1} band is certainly satisfying. Again, comparing the benzenium ion fingerprint spectrum reported here to the IRMPD spectrum,[9] we find substantial differences. In the first report of the IRMPD benzenium ion spectrum, Maître

and co-workers noted that, although a band in the 1600 cm^{-1} region was predicted by DFT calculations, no evidence for this spectral feature was observed. More recently, improvements to the sensitivity of the method allowed for the observation of a very weak band centered at 1581 cm^{-1}.[32] Once again, the feature in the IRMPD spectrum is red-shifted from the intense 1607 cm^{-1} band observed here. Furthermore, the 1581 cm^{-1} band in the IRMPD spectrum is approximately 200 times less intense than the 1433 cm^{-1} transition, in contrast to the ratio predicted by DFT, namely, 0.4:1. For protonated benzene and protonated naphthalene,[32] the lack of intensity for the higher frequency band has been identified as another complication resulting from the multiphoton fragmentation processes associated with IRMPD. In comparison, the relative intensities for the 1456 and 1607 cm^{-1} bands obtained here with Ar tagging and single photon absorption are in excellent agreement with the DFT prediction.

Another set of intense features in the fingerprint region corresponds to a doublet of peaks centered at 1239 and 1198 cm^{-1}. The DFT calculations predict two bands in this region associated with the scissor motion of the CH_2 group. Below 1150 cm^{-1}, several weaker features are observed that are assigned to CH bending modes and a symmetric ring breathing motion. Detailed assignments of all the experimental bands are given in Table 1. Although the previously reported IRMPD spectrum contained a 50 cm^{-1} broad, unresolved band centered at 1237 cm^{-1}, no other transitions were observed below 1200 cm^{-1}.[8d,9] Maître and co-workers have recently noted that transitions with calculated intensities <50 km/mol are frequently missing in the IRMPD spectra of ions isolated in their ICR apparatus.[32,33] In contrast, fragmentation of the rare gas tagged benzenium ion is efficient for even the weak vibrational transitions below 1100 cm^{-1}, which all have calculated transition intensities below 20 km/mol. Given the demonstrated sensitivity and excellent agreement between the experimental and theoretical transition intensities, rare gas tagging and single photon photofragmentation is an effective method for probing the IR fingerprint region of benzenium ions.

Turning our attention to the high frequency region of the spectrum, we find two groups of bands near 2800 and 3000 cm^{-1}. In a previous IRPD study of the $C_6H_7^+Ar$ complex,[8b] Solcà and Dopfer also observed a group of bands centered at 2800 cm^{-1}, along with a weak feature at 3100 cm^{-1}. These bands were assigned to the CH stretches associated with the methylene carbon (sp^3 hybridized) and ring carbons (sp^2 hybridized), respectively. The IRPD spectrum reported here has better sensitivity, revealing four resolved bands in the ring carbon CH stretch region, along with other weaker features to the red and blue of the intense group of bands centered at 2800 cm^{-1}. The four experimental bands associated with the sp^2 carbon CH stretches are observed over a broader frequency range than those predicted by DFT. Nevertheless, this region corresponds to the $(\nu_{13} + \nu_{16})/(\nu_2 + \nu_{16} + \nu_{18})/(\nu_{12})$ Fermi triad region in neutral benzene, and the vibrational complexity observed here may be due to a similar anharmonic resonance involving the four CH stretches and combinations of CC stretches and CH bends. The resonances associated with the aliphatic asymmetric and symmetric CH_2 stretch modes are at lower frequency near 2800 cm^{-1}. In fact, this group of bands corresponds to three sharp, partially resolved features. In the previous study by Solcà and Dopfer, the two weaker bands were attributed to the CH_2 stretches, and the most intense band of the three was assigned to the overtone of a CC ring stretch vibration. This assignment was based on the analogous spectra for the $C_6H_6D^+$ and $C_6D_6H^+$ isotopologues. These authors suggested that, upon ring deuteration, the intense overtone band was shifted outside the region measured, namely, 2700−2900 cm^{-1}. With the 750−3400 cm^{-1} spectrum presented here, we can now identify the transition previously assigned to the overtone of the asymmetric CCC stretch. The associated fundamental corresponds to the band at 1456 cm^{-1}. However, in contrast to the previous suggestion, the 1456 cm^{-1} band is red-shifted by only 15 cm^{-1} upon full deuteration (see Figure S6), and no evidence for the shifted overtone transition is observed below 2700 cm^{-1}. We therefore provide alternative explanations for the third band in the 2800 cm^{-1} region. One alternative explanation is that the band does not simply correspond to an overtone transition but is instead a member of a resonance polyad involving the CCC asymmetric stretch overtone. Assuming the CCC asymmetric stretch overtone borrows intensity from the CH_2 stretch fundamentals, even a small shift upon deuteration may detune the resonance such that the overtone transition is no longer observable. We also note that, although the fingerprint region of the spectrum is largely unaffected by the presence of Ar, the benzenium ion CH_2 stretches are shifted by as much as 24 cm^{-1}. The DFT calculations predict a 50 cm^{-1} splitting between the symmetric and asymmetric stretch bands in the bare ion and a 8.5 cm^{-1} splitting for the complex. Given this sensitivity to the presence of Ar, multiple isomers with respect to the binding location of the Ar may also lead to additional transitions in the 2800 cm^{-1} region. As shown in the Supporting Information, two isomers are found to be stable with similar complexation energies, namely 180 and 210 cm^{-1}. Although four distinct CH_2 stretch bands are predicted for the two isomers, a definitive assignment of the three experimentally resolved features to multiple isomers is precluded due to the inaccuracy associated with the harmonic frequency calculations.

Finally, we compare the gas phase IR spectrum of the benzenium ion reported here to the IR spectrum of a 77 K solid $C_6H_7^+GaCl_4^-$ matrix measured in 1964 by Perkampus and Baumgarten.[4] At the bottom of Figure S19, the matrix intensities and frequencies are reproduced as a stick spectrum. Certainly the gas phase spectrum has considerably better sensitivity and resolution; nevertheless, the number, positions, and relative intensities of the bands in the fingerprint region (700−1700 cm^{-1}) are in excellent agreement. From this we can conclude that the low temperature magic acid matrix minimally perturbs the benzenium ion structure, confirming the applicability of the conclusions drawn from the early landmark studies[3,4] of alkyl substituted benzenium ions to the gas phase species.

The IRPD spectrum of the $C_7H_9^+$ toluenium ion is shown in Figure 3, and the band positions and assignments are given in Table 2. For comparison, the B3LYP spectra are also shown for the four possible structural isomers (**2** through **5**). The relative energies of the four toluenium isomers are given in Table S1, with the para isomer (**5**) being lowest in energy. The ortho (**3**), meta (**4**) and ipso (**2**) isomers are 1.2, 5.0 and 8.8 kcal/mol higher in energy, respectively. The relative energetics computed here are consistent with previous theoretical studies of protonated toluene.[34,35] From the ^{13}C NMR data, Olah observed the lowest energy para isomer to be the dominant structure in the 176 K superacid matrix.[3c] More recently, solid carborane superacids have been used to obtain the structure of the toluenium ion with X-ray crystallography.[36] These studies also determined the para isomer to be the dominant structure. In the gas phase, the isolation of toluenium ions in a 300 K ICR cell coupled to a free electron laser provided IRMPD spectra consistent with a mixture of ortho and para isomers.[35]

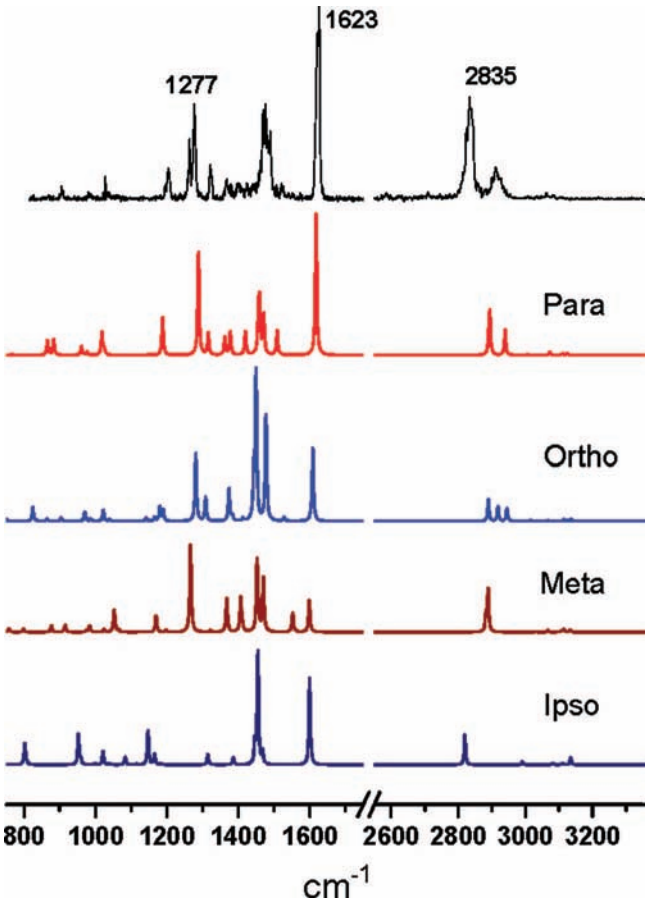

Figure 3. IR photodissociation spectrum of the $C_7H_9^+Ar$ complex measured in the elimination of Ar channel. The simulated spectra from density functional calculations (B3LYP/6-311+G(d,p)) are shown for the para (red), ortho (blue), meta (wine), and ipso (navy) structural isomers of the toluenium ion.

As shown in Figure S16, the fingerprint region of the para isomer spectrum is largely unchanged upon complexation of the toluenium ion with Ar. In comparison to the benzenium ion fingerprint region, for toluenium, there is an onset of spectral congestion in the 1300 to 1500 cm^{-1} region due to bending and twisting modes associated with the methyl group. The intense feature at 1623 cm^{-1} is assigned similarly to the 1607 cm^{-1} band in the benzenium ion spectrum. Once again, a normal mode description of this band corresponds to asymmetric CCC stretching motions of the ring carbons ortho, meta, and para to the methylene, CH_2 group. Interestingly, this band remains sharp and intense in the spectra of protonated *o*-, *m*-, and *p*-xylene as well, with each band falling within the range 1607−1630 cm^{-1} (see Figure S18). As noted above, this spectral feature is indicative of the allylic π-electron density associated with the benzenium ion, and it is apparently characteristic of alkyl substituted benzenium ions in general. The IRPD spectrum in Figure 3 suggests that the para isomer of protonated toluene is the only structure produced here. Close examination reveals that the spectrum predicted by DFT for *p*-$C_7H_9^+$−Ar is quite sufficient to account for all the bands observed and their relative intensities throughout the spectrum. The agreement between the IRPD spectrum and theory is excellent, with essentially all the spectral features reproduced in the simulation. Unfortunately, because many of the strong vibrational bands for the ortho isomer also occur at about the same position as those for the para, we cannot completely exclude the presence of a small concentration of this species. Apparently, however, the collisional cooling in the supersonic expansion is sufficient to anneal the vast majority of $C_7H_9^+$−Ar ions to the globally stable para isomer. The absence of higher energy isomers is in agreement with the low temperature superacid matrix experiments.[3c]

The strong bands near 1607 and 1623 cm^{-1} for the benzenium and toluenium ions, and the similar bands for their analogues, are intriguing with regards to the unidentified infrared bands (UIBs) of interstellar dust. Indeed, Hudgins and co-workers first noted the overlap between the ~1620 cm^{-1} spectral feature predicted for protonated PAHs and the problematic 6.2 μm (1613 cm^{-1}) UIB.[11] Their DFT calculations indicate that this intense spectral signature also persists for polycyclic systems at least as large as protonated circumcoronene.[11] This theoretical result is particularly relevant, because closed shell protonated PAH ions have been shown experimentally to be relatively unreactive toward further hydrogenation reactions.[10] These reactivity studies strongly suggest that the protonated form of PAHs should be abundant in the interstellar carbon-containing gas clouds from which the UIBs are observed.[19c] In addition to the systems presented here, we have observed in preliminary IRPD work an intense feature for protonated naphthalene at 1620 cm^{-1}.[37] Dopfer and co-workers also noted the potential UIB overlap regarding a broad, weak feature at 1599 cm^{-1} in the IRMPD spectrum of protonated naphthalene.[32] From the previous reactivity studies and the IR spectroscopy presented here, it is reasonable to assign the 6.2 μm UIB to carbon ring vibrations associated with protonated PAHs having the characteristic allylic π-bonding moiety seen here.

Conclusions

$C_6H_7^+$ and $C_7H_9^+$ ions are produced in a pulsed discharge cluster source and collisionally cooled in a supersonic expansion. The ion source also produces weakly bound complexes of these ions with Ar. The structures of these ions are probed with IR photodissociation spectroscopy employing the method of rare gas tagging. Careful DFT studies show that the spectra of the argon-tagged ions are essentially the same as those of the free gas phase ions. The low temperature here, and the essentially perturbation-free one-photon spectroscopy allowed by rare gas tagging, enable a detailed assignment of the IR spectrum in the 750−3400 cm^{-1} region. Using either benzene or toluene as precursors, the globally stable benzenium and *p*-toluenium isomers are observed exclusively. The gas phase IRPD spectrum is compared to a previous superacid matrix IR study of solid $C_6H_7^+GaCl_4^-$ at 77 K. The structures of $C_6H_7^+$ ions in the two distinctly different environments are apparently similar, given the similarity of the band origins and intensities of the IR spectra in the fingerprint region.

In the present spectra of both protonated benzene and toluene, a band near 1610 cm^{-1} is assigned to an asymmetric CCC stretch motion of the six membered ring. This band serves as a general marker band for the allylic π-electron density associated with benzenium and alkyl substituted benzenium ions. The 1610 cm^{-1} spectral signature is also predicted to be an intense feature for protonated PAH ions.[11] Given the predicted abundance of these ions in interstellar carbon containing gas clouds,[10] it is reasonable to assign the 6.2 μm (1613 cm^{-1}) UIB to this characteristic signature of the allylic π-electron density.

Acknowledgment. We gratefully acknowledge support for this work from the National Science Foundation (M.A.D, grant no. CHE-0551202; P.v.R.S., grant no. CHE-0716718).

Supporting Information Available: Full details of the DFT and *ab initio* computations done in support of the spectroscopy

here, including the structures, energetics and vibrational frequencies for each of the structures considered and spectra. This material is available free of charge *via* the Internet at http://pubs.acs.org.

References and Notes

(1) (a) Olah, G. A. *Acc. Chem. Res.* **1971**, *4*, 240. (b) March, J. *Advanced Organic Chemistry: Reactions, Mechanisms, and Structure*; McGraw Hill: New York, 1977; pp 453−519. (c) Brouwer, D. M.; Mackor, E. L.; MacLean, C. In *Carbonium Ions*; Olah, G. A., Schleyer, P. v. R., Eds.; John Wiley and Sons: New York, 1970; pp 837−897. (d) Shubin, V. G.; Borodkin, G. I. In *Carbocation Chemistry*; Olah, G. A., Prakash, G. K. S. Eds.; John Wiley and Sons: Hoboken, NJ, 2004; pp 125−141.

(2) (a) Doering, W.v. E.; Saunders, M.; Boyton, H. G.; Earhart, H. W.; Wadley, E. F.; Edwards, W. R.; Laber, G. *Tetrahedron* **1958**, *4*, 178. (b) Dallinga, G.; Mackor, E. L.; Stuart, A. A.V. *Mol. Phys.* **1958**, *1*, 123. (c) MacLean, C.; Mackor, E. L. *Mol. Phys.* **1961**, *4*, 241. (d) MacLean, C.; Mackor, E. L. *Discuss. Faraday Soc.* **1962**, *34*, 165. (e) Birchall, T.; Gillespie, R. J. *Can. J. Chem.* **1964**, *42*, 502.

(3) (a) Olah, G. A. *J. Am. Chem. Soc.* **1965**, *87*, 1103. (b) Olah, G. A.; Schlosberg, R. H.; Kelly, D. P.; Mateescu, Gh. D. *J. Am. Chem. Soc.* **1970**, *92*, 2546. (c) Olah, G. A.; Schlosberg, R. H.; Porter, R. D.; Mo, Y. K.; Kelly, D. P.; Mateescu, G. D. *J. Am. Chem. Soc.* **1972**, *94*, 2034. (d) Olah, G. A.; Staral, J. S.; Asencio, G.; Liang, G.; Forsyth, D. A.; Mateescu, G. D. *J. Am. Chem. Soc.* **1978**, *100*, 6299.

(4) Perkampus, H. H.; Baumgarten, E. *Angew. Chem., Int. Ed.* **1964**, *3*, 776.

(5) (a) Gold, V.; Tye, F. L. *J. Chem. Soc.* **1952**, 2172. (b) Reid, C. *J. Am. Chem. Soc.* **1954**, *76*, 3264.

(6) (a) Williams, D. H.; Hvistendahl, G. *J. Am. Chem. Soc.* **1975**, *96*, 6755. (b) Hvistendahl, G.; Williams, D. H. *J. Chem. Soc., Perkin Trans.* **1975**, *2*, 881. (c) Bruins, A. P.; Nibbering, N. M. M. *Org. Mass. Spectrom.* **1976**, *11*, 950. (d) Lau, Y. K.; Kebarle, P. *J. Am. Chem. Soc.* **1976**, *98*, 7452. (e) Yamdagni, R.; Kebarle, P. *J. Am. Chem. Soc.* **1976**, *98*, 1320. (f) Franchetti, V.; Freiser, B. S.; Cooks, R. G. *Org. Mass Spectrom.* **1978**, *13*, 106. (g) Hartman, K. G.; Lias, S. G. *Int. J. Mass Spectrom. Ion Phys.* **1978**, *28*, 213. (h) Bohme, D. K.; Stone, J. A.; Mason, R. S.; Stradling, R. S.; Jennings, K. R. *Int. J. Mass Spectrom. Ion Phys.* **1981**, *37*, 283. (i) Ausloos, P.; Lias, S. G. *J. Am. Chem. Soc.* **1981**, *103*, 3641. (j) Lias, S. G.; Ausloos, P. *J. Chem. Phys.* **1985**, *82*, 3613. (k) Kuck, D.; Ingemann, S.; de Koning, L. J.; Grutzmacher, H.-F.; Nibbering, N. M. M. *Angew. Chem., Int. Ed. Engl.* **1985**, *24*, 693. (l) Kuck, D.; Schneider, J.; Grutzmacher, H.-F. *J. Chem. Soc., Perkin Trans. 2* **1985**, 689. (m) Mason, R. S.; Fernandez, M. T.; Jennings, K. R. *J. Chem. Soc., Faraday Trans.* **1987**, *83*, 89. (n) McMahon, A. W.; Chadikun, F.; Harrison, A. G.; March, R. E. *Int. J. Mass Spectrom. Ion Processes* **1989**, *87*, 275. (o) Kuck, D. *Mass Spectrom. Rev.* **1990**, *9*, 583. (p) Parry, A.; Fernandez, M. T.; Garley, M.; Mason, R. *J. Chem. Soc., Faraday Trans.* **1992**, *88*, 3331. (q) Petrie, S.; Javahery, G.; Bohme, D. K. *J. Am. Chem. Soc.* **1992**, *114*, 9205. (r) Gaumann, T.; Zhao, Z.; Zhu, Z. *Rapid Commun. Mass Spectrom.* **1994**, *8*, 1. (s) Chiavarino, B.; Crestoni, M. E.; DePuy, C. H.; Fornarini, S.; Gareyev, R. *J. Phys. Chem.* **1996**, *100*, 16201. (t) Chiavarino, B.; Crestoni, M. E.; Fornarini, S. *J. Phys. Org. Chem.* **2004**, *17*, 957. (u) McLain, J. L.; Poterya, V.; Molek, C. D.; Babcock, L. M.; Adams, N. G. *J. Phys. Chem. A* **2004**, *108*, 6704.

(7) (a) Freiser, B. S.; Beauchamp, J. L. *J. Am. Chem. Soc.* **1976**, *98*, 3136. (b) Freiser, B. S.; Beauchamp, J. L. *J. Am. Chem. Soc.* **1977**, *99*, 3214.

(8) (a) Solcà, N.; Dopfer, O. *Chem. Phys. Lett.* **2001**, *342*, 191. (b) Solcà, N.; Dopfer, O. *Angew. Chem., Int. Ed.* **2002**, *41*, 3628. (c) Solcà, N.; Dopfer, O. *Chem. Eur. J.* **2003**, *9*, 3154. (d) Dopfer, O.; Solcà, N.; Lemaire, J.; Maître, J.; Crestoni, M. E.; Fornarini, S. *J. Phys. Chem. A* **2005**, *109*, 7881. (e) Solcà, N.; Dopfer, O. *ChemPhysChem* **2005**, *6*, 434. (f) Dopfer, O. *J. Phys. Org. Chem.* **2006**, *19*, 540.

(9) Jones, W.; Boissel, P.; Chiavarino, B.; Crestoni, M. E.; Fornarini, S.; Lemaire, J.; Maître, P. *Angew. Chem., Int. Ed.* **2003**, *42*, 2057.

(10) (a) Le Page, V.; Keheyan, Y.; Bierbaum, V. M.; Snow, T. P. *J. Am. Chem. Soc.* **1997**, *119*, 8373. (b) Snow, T.; Le Page, V.; Keheyan, Y.; Bierbaum, V. M. *Nature* **1998**, *391*, 259.

(11) (a) Hudgins, D. M.; Bauschlicher.; Jr, C. W.; Allamandola, L. J. *Spectrochim. Acta, Part A* **2001**, *57*, 907. (b) Beegle, L. W.; Wdowiak, T. J.; Harrison, J. G. *Spectrochim. Acta, Part A* **2001**, *57*, 737.

(12) Pfeiffer, P.; Wizinger, R. *Liebigs Ann. Chem.* **1928**, *461*, 132.

(13) Wheland, G. W. *J. Am. Chem. Soc.* **1942**, *64*, 900.

(14) Muller, N.; Pickett, L. W.; Mulliken, R. S. *J. Am. Chem. Soc.* **1954**, *76*, 4770.

(15) McCaulay, D. A.; Lien, A. P. *J. Am. Chem. Soc.* **1951**, *73*, 2013.

(16) (a) Hehre, W. J.; Pople, J. A. *J. Am. Chem. Soc.* **1972**, *94*, 6901. (b) Hehre, W. J.; McIver, R. T.; Pople, J. A.; Schleyer, P.v. R. *J. Am. Chem. Soc.* **1974**, *96*, 7162. (c) Ermler, W. C.; Mulliken, R. S.; Clementi, E. *J. Am. Chem. Soc.* **1976**, *98*, 388.

(17) (a) Siebler, S.; Schleyer, P. v. R.; Gauss, J. *J. Am. Chem. Soc.* **1993**, *115*, 6987. (b) Howard, S. T.; Wozniak, K. *Chem. Phys. Lett.* **1993**, *212*, 1. (c) Glukhovtsev, M. N.; Pross, A.; Nicolaides, A.; Radom, L. *J. Chem. Soc., Chem. Commun.* **1995**, 2347. (d) Maksić, Z. B.; Kovačević, B.; Lesar, A. *Chem. Phys.* **2000**, *253*, 59. (e) Dill, J. D.; Schleyer, P.v. R.; Binkley, J. S.; Seeger, R.; Pople, J. A.; Haselbach, E. *J. Am. Chem. Soc.* **1976**, *98*, 5428.

(18) Cravens, T. E.; Robertson, I. P., Jr.; Wait, J. H.; Yelle, R. V.; Kasprzak, W. T.; Keller, C. N.; Ledvina, S. A.; Niemann, H. B.; Luhmann, J. G.; McNutt, R. L.; Ip, W.-H.; De La Haye, V.; Mueller-Wodarg, I.; Wahlund, J.-E.; Anicich, V. G.; Vuitton, V. *Geophys. Res. Lett.* **2006**, *33*, L07105.

(19) (a) Allamandola, L. J.; Tielens, A. G. G. M.; Barker, J. R. *Astrophys. J. Suppl. Series* **1989**, *71*, 733. (b) Joblin, C. *Faraday Discuss.* **1998**, *109*, 349. (c) Peeters, E.; Hony, S.; Van Kerckhoven, C.; Tielens, A. G. G. M.; Allamandola, L. J.; Hudgins, D. M. *Astron. Astrophys.* **2002**, *390*, 1089.

(20) (a) Yeh, L. I.; Okumura, M.; Myers, J. D.; Price, J. M.; Lee, Y. T. *J. Chem. Phys.* **1989**, *91*, 7319–7330. (b) Okumura, M.; Yeh, L. I.; Myers, J. D.; Lee, Y. T. *J. Phys. Chem.* **1990**, *94*, 3416.

(21) Ebata, T.; Fujii, A.; Mikami, N. *Int. Rev. Phys. Chem.* **1998**, *17*, 331.

(22) Bieske, E. J.; Dopfer, O. *Chem. Rev.* **2000**, *100*, 3963.

(23) Robertson, W. H.; Johnson, M. A. *Annu. Rev. Phys. Chem.* **2003**, *54*, 173.

(24) Duncan, M. A. *Int. Rev. Phys. Chem.* **2003**, *22*, 407.

(25) (a) Douberly, G. E.; Ricks, A. M.; Ticknor, B. W.; Duncan, M. A. *J. Phys. Chem. A* **2008**, *112*, 950. (b) Douberly, G. E.; Ricks, A. M.; Ticknor, B. W.; McKee, W. C.; Schleyer, P. v. R.; Duncan, M. A. *J. Phys. Chem. A* **2008**, *112*, 1897.

(26) Bosenberg, W. R.; Guyer, D. R. *J. Opt. Soc. Am. B* **1993**, *10*, 1716.

(27) (a) Schmidt, M. W.; Baldridge, K. K.; Boatz, J. A.; Elbert, S. T.; Gordon, M. S.; Jensen, J. H.; Koseki, S.; Matsunaga, N.; Nguyen, K. A.; Su, S.; Windus, T. L.; Dupuis, M.; Montgomery, J. A. *J. Comput. Chem.* **1993**, *14*, 1347. (b) Gordon, M. S.; Schmidt, M. W. In *Theory and Applications of Computational Chemistry: The First Forty Years*; Dykstra, C. E., Frenking, G., Kim, K. S., Scuseria, G. E. Eds.; Elsevier: Amsterdam, 2005; pp 1167.

(28) Scott, A. P.; Radom, L. *J. Phys. Chem.* **1996**, *100*, 16502.

(29) Moran, D.; Simmonett, A. C., III; Allen, W. D.; Schleyer, P.v. R.; Schaefer, H. F., III *J. Am. Chem. Soc.* **2006**, *128*, 9342.

(30) (a) Douberly, G. E.; Ricks, A. M.; Ticknor, B. W.; Schleyer, P. v. R.; Duncan, M. A. *J. Am. Chem. Soc.* **2007**, *129*, 13782. (b) Douberly, G. E.; Ricks, A. M.; Schleyer, P. v. R.; Duncan, M. A. *J. Chem. Phys.* **2008**, *128*, 021102. and references cited.

(31) Oomens, J.; Sartakov, B. G.; Meijer, G.; von Helden, G. *Int. J. Mass Spectrom* **2006**, *254*, 1.

(32) Lorenz, U. J.; Solcà, N.; Lemaire, J.; Maître, P.; Dopfer, O. *Angew. Chem., Int. Ed.* **2007**, *46*, 6714.

(33) Lorenz, U. J.; Lemaire, J.; Maître, P.; Crestoni, M. E.; Fornarini, S.; Dopfer, O. *Int. J. Mass Spectrom.* **2007**, *267*, 43.

(34) Ishikawa, Y.; Yilmaz, H.; Yanai, T.; Nakajima, T.; Hirao, K. *Chem. Phys. Lett.* **2004**, *396*, 16.

(35) Dopfer, O.; Lemaire, J.; Maître, P.; Chiavarino, B.; Crestoni, M. E.; Fornarini, S. *Int. J. Mass Spectrom.* **2006**, *249−250*, 149.

(36) Reed, C. A.; Kim, K.-C.; Stoyanov, E. S.; Stasko, D.; Tham, F. S.; Mueller, L. J.; Boyd, P. W. D. *J. Am. Chem. Soc.* **2003**, *125*, 1796.

(37) Douberly, G. E.; Ricks, A. M.; Duncan, M. A. Unpublished results. The intense 1620 cm^{-1} IRPD band observed for the protonated naphthalene−Ar complex should be compared to a 15 cm^{-1} broad, weak feature observed at 1599 cm^{-1} in the IRMPD spectrum of the bare protonated naphthalene ion (see ref 32).

JP802020N